Available online at www.sciencedirect.com
SCIENCE DIRECT®
Forest Ecology and Management 212 (2005) 50–64
Forest Ecology and Management
www.elsevier.com/locate/foreco

Evaluating the use of remotely sensed data in matrix population modeling for eastern hemlock (*Tsuga canadensis* L.)

W. Robert Lamar *, James B. McGraw

Department of Biology, West Virginia University, Morgantown, WV 26506-6057, USA

Received 16 November 2004; received in revised form 26 February 2005; accepted 28 February 2005

Abstract

Matrix population models for a population of eastern hemlock (*Tsuga canadensis* L.) were constructed from population data collected on the ground using traditional field methods and analogous data extracted from low elevation aerial imagery. This aerial derived data was obtained using spectral and spatial segmentation and reconciliation procedures that segmented hemlock ''blobs'' from the forest canopy image. Fertility estimates in the aerial derived matrix model were obtained using the spatially explicit nature of remotely sensed data, including functions relating fertility to both parental size and distance between prospective parent and newborn. Matrix analysis produced a number of useful population characteristics including overall population growth rate (λ), stable stage distributions, reproductive values, and elasticity values. λ's calculated from the aerial and ground derived matrices were compared using randomization tests. λ's from both aerial and ground derived matrices showed significant increases in population growth rate from the 1997–1998 to the 1998–1999 census periods. Other data measured from the aerial imagery and on the ground seemed to support this population change, the result of a damaging February 1998 ice storm. While providing a perspective and description of a population that differs from traditional ground approaches, demographic studies using remote sensing provide some promising advantages. The spatially explicit nature of the data permits more biologically realistic modeling of the population and the investigation of potential environmental influences on population dynamics. Automated extraction of demographic or megademographic data from remotely sensed images represents an important first step toward scaling population analysis to the landscape and regional levels.
© 2005 Elsevier B.V. All rights reserved.

Keywords: Matrix population model; Hemlock; Remote sensing; Population growth rate; Demography; Spatially explicit population data; Fertility probabilities

1. Introduction

Over the past two decades, the study of plant demography has evolved from a largely descriptive exercise with limited samples to a powerful tool with applications in forestry (Freckleton et al., 2003), conservation biology (Menges, 1990; Allphin and

* Corresponding author.
E-mail addresses: rlamar@swva.net (W.R. Lamar), jmcgraw@wvu.edu (J.B. McGraw).

0378-1127/$ – see front matter © 2005 Elsevier B.V. All rights reserved.
doi:10.1016/j.foreco.2005.02.056

Harper, 1997; Kaye et al., 2001), invasive species ecology (Golubov et al., 1999; Parker, 2000), plant–pathogen interactions (Davelos and Jarosz, 2004), and disturbance ecology (Silvia et al., 1991; Baptista et al., 1998). An array of demographic modeling approaches may be taken once adequate census data are available, ranging from individual-based models to size- or stage-based matrix models. Matrix population models are frequently used in plant demographic studies due, in part, to the number of informative statistics provided by matrix analysis (Silvertown et al., 1996).

Interactions among plants are localized, hence, population dynamics are inherently spatial (Pacala, 1989). In recent years, spatially explicit population models have become increasingly important in the study of population dynamics in heterogeneous environments (Shugart and Smith, 1992; Busing, 1995; Dunning et al., 1995; Pacala et al., 1996). One of the chief disadvantages of such models is the difficulty of obtaining spatially explicit population data in the field (Dunning et al., 1995). Indeed, despite the many advances in plant demography, demographic studies of plants remain limited in scope ($n < 10{,}000$) because of the labor required to census and map populations (Silvertown et al., 1996). Yet many ecological questions, particularly those concerning regional or global species status changes, could benefit from more intensive and spatially explicit sampling of populations.

Remote sensing allows the collection of large amounts of spatially explicit information over a large geographic area in a short amount of time; potentially useful characteristics when studying plant population dynamics. At present, high spatial resolution imagery provided by aircraft-based photographic systems appears to provide data at a scale most feasible for the collection of population level demographic data (Gougeon, 1995; Niemann, 1995; Wulder et al., 2000; Erikson, 2003), although recently launched space-based platforms (i.e. IKONOS and QuickBird) are approaching the resolution (ca. 1 m) required to discern individuals (Kramer, 2002).

The challenge to an ecologist is how to adapt the traditional methods of description and classification to be compatible with the nature of remotely sensed data (Graetz, 1990). The basic unit traditionally used to describe populations has been the individual. In the construction of a matrix model, matrix elements usually describe the transition probability of individuals between life stages. Yet the modular, as opposed to unitary, construction of most plants has long been recognized (Harper, 1976). Using this modular approach the fundamental unit of a plant population may be regarded as any repeating unit of construction such as a tree branch or branches (Huenneke and Marks, 1987; McGraw, 1989), tree blobs (Lamar et al., 2004), pixels (Hall et al., 1991), or spatial units (Guardia et al., 2000). In the case of blobs observed in aerial images, a ‘‘tree blob’’ is defined as a distinct portion of crown canopy segmented from its neighbors on the basis of size, shape, and connectivity. Using automated segmentation and reconciliation procedures, a population of eastern hemlock (*Tsuga canadensis* L.) blobs has been previously described and censused over a 3-year period (Lamar et al., 2004) This spatially explicit, multitemporal data set provides a different perspective with which to investigate population dynamics and influences.

In this paper, we constructed two matrix population models for a population of hemlock. Parameters for one of these models were estimated from demographic data collected on the ground using traditional field methods. Parameters for the other model were estimated from demographic data extracted from low elevation aerial imagery. The results of these aerial and ground derived matrices were compared. The usefulness of matrix models constructed from remotely sensed data to detect and quantify population change and assist in the understanding of the causes of change was evaluated.

2. Materials and methods

2.1. Study plot

The 3 ha (100 m × 300 m) study plot was located in the Limberlost-Whiteoak Canyon area of Shenandoah National Park (38°34′N 78°22′W) in an upper elevation (951 m) mixed hardwood/hemlock forest. Hemlock is a long-lived, shade-tolerant, evergreen tree found in many low disturbance eastern United States (US) forests. Established populations usually include a large bank of ‘‘saplings,’’ small individuals that may be suppressed beneath a canopy of hemlock or hardwoods for hundreds of years and remain in

good condition (Godman and Lancaster, 1990). Hemlock seed ripening and dispersal coincides with the cones changing to a deep brown color in the fall. Seeds require a chilling period prior to germination. Spring germination is seldom delayed because of seed dormancy (Godman and Lancaster, 1990).

2.2. Data set development—ground

Hemlock trees within the plot were censused in the early spring of 1997–1999. All hemlock trees ($n = 1438$ within the study plot) with a diameter at breast height (dbh, breast height = 1.3 m) ≥ 5.0 cm were tagged and measured (dbh).

Within the study plot, four 20 m $\times$ 20 m sub-plots were randomly established and all smaller hemlocks (dbh < 5.0 cm) were tagged. The dbh of all hemlocks in the sub-plots was measured. Trees too small to have a central bole at breast height were measured by height from ground to the topmost branch of its crown. All measurements of hemlock < 5 cm were taken in April of 1997–1999. The numbers of new recruits within the four random sub-plots were counted in 1998 and 1999.

2.3. Data set development—remote sensing

Large scale (1:3000) color aerial photographs of the study plot were collected on 27 March 1997, 13 April 1998, and 31 March 1999 using a calibrated Leica/Wild Heerbrugg RC-30 mapping camera with a 303.860 mm focal-length lens. The photography was acquired before the emergence of new foliage for the deciduous forest component. The color photographs were scanned at 600 dpi to produce high resolution ($\sim$13 cm/pixel) digital images (Fig. 1a). With shared primary branch bifurcation points identified throughout the image segment as control points, images were co-registered using second order mapping polynomials and cubic convolution resampling (Lamar et al., 2004).

The evergreen vegetation of the study plot was spectrally segmented from other ground covers. Spectral segmentation was completed using a maximum likelihood classification algorithm and a global, fused class decision making process (Lamar, 2003). Due to the relatively coarse spectral resolution of the sensor and the overlapping spectral signatures of the four evergreen components in the study plot (hemlock, *Tsuga Canadensis*; mountain laurel, *Kalmia latifolia*; red spruce, *Picea rubens*; white pine, *Pinus strobus*) we were unsuccessful in spectrally differentiating the evergreen species. A 1998 crown survey, performed by manually delineating individual hemlock crowns on the ground assisted by multiple years of aerial imagery and multiple images from different viewing angles each year, showed that $\sim$97% of the evergreen component in the study plot was hemlock (Lamar, 2003). Based on this finding, we will hereafter inclusively refer to the evergreen component as the hemlock component. The consequences of this broad labeling will be discussed later.

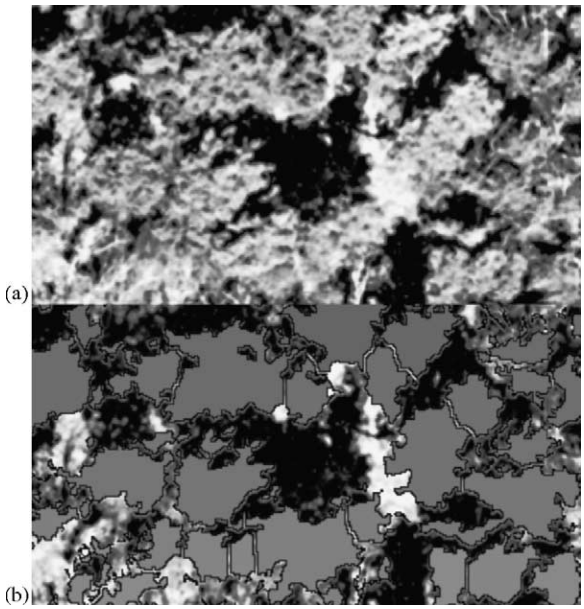

Fig. 1. (a) Aerial view of portion of study site and (b) same aerial view with hemlock blobs delineated using spectral and spatial segmentation procedures.

For multitemporal image comparisons, the presence of crown shadows presented a challenge. The occurrence of shadows over an area masked the true nature of the ground cover. For example, if a particular area was classified as hemlock at time t and shadow at time $t + 1$, the shadows could be masking hemlock in which case no actual change had occurred, or the shadow could be masking an actual change between hemlock and another ground cover. Because of the classification uncertainty of pixels exhibiting shadow/hemlock transitions between time periods, we chose to

eliminate those pixels from consideration prior to further image processing and comparison. As a result, any pixel that had been classified as shadow at any time in a multitemporal same scene data set was reclassified as shadow at all times. While the compounding of shadows amplified the masking of information about the true nature of the ground cover, comparing only two images at a time minimized this effect. Thus, 1997 and 1998 shadows were added to both images within the 1997–1998 image pair and 1998 and 1999 shadows were added to both images of the 1998–1999 image pair. This extra shading resulted in an additional 13.5% and 10.3% of the hemlock classified in the 1998 image being masked in shadow in the 1997–1998 and 1998–1999 image pairs, respectively.

The binary image pairs were then independently routed through an automated spatial segmentation and reconciliation procedure that divided the hemlock component of the images into individual population units or blobs (Fig. 1b) based on size, shape, and connectivity (Lamar et al., 2004). Processing the aerial imagery through these procedures resulted in the production of two paired data sets, maps of unique, spatially explicit hemlock blobs from 1997–1998 and from 1998–1999.

2.4. Matrix model

A stage (size) structured matrix population model (Lefkovich, 1965) was used to describe the population dynamics of the hemlock population based on both ground and aerial data sets. This model projected the size and structure of a population from time t to time $t + 1$ as:

$$\mathbf{n}(t+1) = \mathbf{A}\mathbf{n}(t) \tag{1}$$

where $\mathbf{n}$ was a vector whose entries represented the number of population units (individuals for the ground data and blobs for the aerial data) within each size class and $\mathbf{A}$ was the projection matrix whose elements a_{ij} were transition probabilities; the number of population units in size class i at time $t + 1$ per unit in size class j at time t. Analysis of the matrix $\mathbf{A}$ provided a number of useful population characteristics. The dominant eigenvalue (λ) of $\mathbf{A}$ yielded the long-term population growth rate, assuming transition probabilities were constant over time. The right eigenvector ($\mathbf{w}$) and left eigenvector ($\mathbf{v}$) corresponding to λ described the stable size distribution (the ultimate proportions of the population in each size class) and the size-specific reproductive values (the relative contribution to future population growth that an individual currently in a particular size class is expected to make) (Caswell, 2001).

Elasticity or proportional sensitivity, values of transition elements measure the response of λ to proportional changes in these transition elements. Elasticity was calculated from Caswell (2001) as:

$$e_{ij} = \frac{a_{ij}}{\lambda} \times \frac{\partial \lambda}{\partial a_{ij}} \tag{2}$$

2.5. Parameter estimates—ground

From the ground data, hemlock individuals were divided into six size classes (1) <5.0 cm dbh, (2) 5.0–10.0 cm dbh, (3) 10.1–17.5 cm dbh, (4) 17.6–27.5 cm dbh, (5) 27.6–42.5 cm dbh, and (6) >42.5 cm dbh. To establish size classes for all adults (individuals $\geq$ 10.1 cm), we used an algorithm developed by Moloney (1986), that minimized both sampling and distribution errors for the 3 years of data.

Estimates of matrix elements representing growth, regression and stasis were obtained using a maximum likelihood estimate of observed transition frequencies (Caswell, 2001) from time t to time $t + 1$ such that

$$a_{ij} = \frac{m_{ij}}{\sum_{i=1}^{s+1} m_{ij}} \tag{3}$$

where s was the number of size classes in the population state vector $\mathbf{n}$, class $s + 1$ corresponded to individuals of a particular class j that died in the year between censuses, and m_{ij} was the number of observed transitions from size class j to fate i from one census to the next. Since sampling of the smallest individuals (size class 1) was limited to the four sub-plots, only one estimate of this class' stasis and growth transitions was calculated by summing observed transitions from all 3 years of population data. This one estimate was used for both 1997–1998 and 1998–1999 ground-based matrix models.

Estimating mean fertility for individuals is challenging for any plant species that produces copious quantities of seed (too many to count), each of which has a very low (difficult to estimate) probability of

germinating and surviving to the subsequent census. Therefore, indirect estimates are typically used to calculate individual fertility probabilities. In this study, an estimate of total number of new recruits per year (M) was obtained by averaging the number of new recruits found in four randomly established 20 m × 20 m plots in 1998 and 1999, and extrapolating to the area of the entire population. Fertility probabilities were then estimated for all adults (dbh ≥ 10 cm) present in the population the previous year as a function of tree size. Both linear (Clark et al., 1998) and exponential (Ribbens et al., 1994) fertility functions of size have been described for hemlock. Pinero et al. (1984) suggested that an exponential increase in fertility with size is the most common pattern found in tree species. We thus estimated fertility probability f of each adult individual k in the population as

$$f_k = \frac{\mathrm{dbh}_k^2}{\sum_k \mathrm{dbh}_k^2} \times M \quad (4)$$

Class fertilities F were calculated from Eq. (4) as

$$F_i = \frac{\sum_k f_k(i)}{N_i} \quad (5)$$

where N is the total number of individuals in size class i.

Fertility estimates represented the average number of new recruits (time $t + 1$) per adult of that size class (i) in the population (time t). The timing of sampling (early spring) meant that ''new'' seedlings had actually survived nearly a year since germination the previous spring. New recruits, thus, reflected both a germination and survival (from birth to the next census) component.

Typically, individuals of a long-lived, low disturbance species such as hemlock experience very little change between census periods. For the 1998–1999 matrix, this lack of change resulted in no mortality for individuals of the largest size class ($a_{66} = 1$). This condition was an artifact of the limited nature of the sampling and was not expected to persist. A more biologically realistic transition was therefore substituted into the matrix for a_{66}. Adjusted mortality for size class 6 individuals was calculated as the averaged mortality of size class 6 (where mortality = 0) and size class 5 individuals, yielding an estimated a_{66} value of 0.9962.

2.6. Parameter estimates—remote sensing

In order to make comparisons between models produced from traditional ground data and remote sensing data, we established corresponding individual and blob size classes as follows. The population of hemlock blobs delineated from aerial imagery was divided into size classes corresponding to the five largest size classes developed for the same population censused on the ground. Class boundaries were determined based on the relationship between dbh of individuals measured on the ground and visible canopy area of individuals measured from aerial images in the 1998 crown survey. This relationship produced a regression equation:

$$\text{visible crown area (in pixels)} = 37.6585 + 28.0415\,(\text{dbh})$$
$$r^2 = 0.60,\ p < 0.0001 \quad (6)$$

Substituting the size class boundaries of the ground data into Eq. (6) produced blob size classes (in pixels) of: (1) 178–318, (2) 319–528, (3) 529–809, (4) 810–1229, and (5) ≥1230. Blobs < 178 pixels presented a challenge. Many of the smallest patches of hemlock visible from the air were found to be separated at such a distance from all identified hemlock crowns that they could not be linked with certainty to any one crown in the 1998 manually delineated crown survey (Lamar, 2003). These smallest patches represented isolated hemlock branches cut off from the main crown by shadows or other ground covers or crowns belonging to hemlocks with a dbh < 5 cm. Because of the uncertain identity and relative insignificance of these smallest patches, all blobs < 178 pixels were considered ''noise'' and eliminated from further comparison and description.

Like the ground data, blob fertility was estimated as a function of parental size. Unlike the ground data, the presence of ''newborn'' blobs within the aerial data sets was not the product of recent germination. Instead, ''newborn'' blobs were defined as all new hemlock blobs visible in image time $t + 1$ but not in image time t. The emergence of these new hemlocks was often the result of a canopy disturbance event that opened a gap in the canopy and allowed the previously hidden hemlock to be visible in the aerial image (i.e. ''born'' into the canopy). As in Eq. (4), we assumed

that fertility followed an exponential pattern with size such that

$$\text{fertility probability}_k \propto \text{crown area}_k^2 \quad (7)$$

In addition to being a function of parental size, fertility is also expected to be a function of the distance from the seed source to the new recruit (Harper, 1977). While individual-based simulation models have incorporated a distance function into estimates of recruitment (Pacala et al., 1996), most matrix projection models do not include such biological realism. The spatially explicit nature of the aerial data set permitted us to model fertility probabilities as a function of both blob size and distance of adult blobs from each new recruit. Only adult blobs present on the previous year's imagery were considered as possible "parents". Adult blobs, as predicted by Eq. (6), were defined as all blobs >318 pixels (i.e. blobs corresponding to trees >10.1 cm dbh). Because most hemlock seed dispersal is within tree height (Godman and Lancaster, 1990), fertility probabilities were estimated only for adult blobs (k) within 30 m of each newly emerged blob.

A number of empirical seed/seedling dispersal functions have been developed for trees. Greene et al. (2004) evaluated three commonly used seed/seedling dispersal functions (lognormal, 2Dt, and the two-parameter Weibull) with relatively minor differences in log likelihood for studies of hemlock seeds, cones, and germinants. Interestingly, dispersal of each of the three hemlock life stages was predicted best by a different dispersal function, lognormal (for germinants), 2Dt (for seeds) and Weibull (for cones). In other studies, the Weibull function was found to produce a higher log likelihood than the 2Dt function for hemlock seeds. (Clark et al., 1999). In our study, we chose to model the seed/seedling dispersal curve of hemlock based on the two-parameter Weibull function (Ribbens et al., 1994). This function predicted that recruitment would follow a Poisson distribution where the mean of the Poisson distribution was determined by the distance between the new recruit and potential parent such that

$$\text{fertility probability} \propto e^{-Dm^S} \quad (8)$$

where D determined the steepness of decline of fertility probability as distance from new recruit increased, S determined the shape of the distribution, and m was the mean distance (in meters) between all pixels of the potential parent and the new recruit. Ribbens et al. (1994) calculated maximum likelihood values for D and S that produced a best fit of field observed and predicted spatial distributions for new recruits. These values of $D = 44.720410 \times 10^{-5}$ and $S = 3$ were substituted into Eq. (8) and used to calculate fertility probabilities.

The relative fertility probability f of each potential hemlock parent blob k with regard to each new recruit l was calculated as the product of the size and distance function such that:

$$f_{kl} = \frac{\text{crown area}_{kl}^2 \times e^{-Dm^3}}{\sum_k \text{crown area}_{kl}^2 \times e^{-Dm^3}} \quad \text{with} \sum_k f_{kl} = 1 \quad (9)$$

Class fertilities F_i are then calculated as

$$F_i = \frac{\sum_{kl} f_{kli}}{N_i} \quad (10)$$

where N_i is the total number of blobs in size class i.

2.7. Statistical comparison

A randomization, or permutation, test was used to assess variation found in λ for the 1997–1998 and 1998–1999 matrices derived from both ground and aerial-based sampling (Caswell, 2001). A test statistic $\theta = |\lambda_t - \lambda_{t+1}|$was used to construct a two-tailed test of the null hypothesis that time had no effect. Data on all individuals from both matrices were randomly resampled without replacement to produce a permuted data set maintaining the original sample sizes for both times. The test statistic $\theta^{(i)}$ was calculated from this ith data set and the process repeated for a sample of 3000 random permutations. The probability, given the H_0, that $\theta \geq \theta_{obs}$ was calculated

$$P[\theta \geq \theta_{obs}|H_0] = \frac{\{\theta^{(i)} \geq \theta_{obs}\} + 1}{3000 + 1} \quad (11)$$

3. Results

Matrix population models were constructed for 1997–1998 and 1998–1999 using both ground and aerial derived census data (Tables 1 and 2). Population characteristics (λ, stable size distribution, reproduc-

Table 1
Hemlock population matrices derived from aerial data sets

Stage at time $t+1$	Stage at time t				
	1	2	3	4	5
1997–1998					
1	0.3766	0.1305	0.0558	0.0824	0.8300
2	0.1948	0.5309	0.0934	0.0413	0.0451
3	0.1299	0.2461	0.6014	0.2763	0.0808
4	0.0260	0.0227	0.2236	0.5408	0.0808
5	0	0	0.0185	0.1504	0.8247
1998–1999					
1	0.3240	0.0954	0.0503	0.0636	0.1307
2	0.1972	0.4721	0.1340	0.0429	0.0934
3	0.0845	0.2956	0.5744	0.2128	0.0753
4	0.0845	0.1147	0.2301	0.6346	0.1784
5	0.0282	0.0377	0.0600	0.1812	0.8129

tive values, and elasticities) calculated from the aerial and ground derived matrices are summarized in Tables 3 and 4. Several of these characteristics showed comparable patterns for both aerial and ground derived matrices. Reproductive values calculated from both type of matrices increased in larger size classes. Both blobs and individuals belonging to the largest size classes are expected to contribute the most to future population growth. The actual reproductive rates associated with the ground censused individuals were much larger than the values linked to aerial censused blobs, reflecting the different definitions of ''newborn'' individuals and ''newborn'' blobs in this study.

Elasticity values also showed similar, although not identical, patterns for both ground and aerial derived matrices. For long-lived tree species, the importance of adult survival is critical and well-documented (Silvertown et al., 1996). It is thus not surprising that the largest elasticity values for both types of matrices were associated with transitions where adults (blobs and individuals) remained in the same size class (i.e. survived) over time.

From 1997 to 1998 data, both population matrices projected a population close to equilibrium, with the ground derived matrix projecting a slightly declining population ($\sim$0.5%) and the aerial derived matrix projecting a slightly increasing population ($\sim$1.0%). From 1998 to 1999 data, both population matrices projected an increasing population, a 1% increase according to the ground data and a $>$9% increase according to the aerial data. Perhaps, most interestingly, between 1997–1998 and 1998–1999, both ground derived and aerial derived population matrices projected a significant increase in λ.

A similar pattern of change between 1997–1998 and 1998–1999 data was found in other descriptions of the hemlock canopy collected in the air and on the ground during this time frame; a change believed to have been triggered by a severe February 1998 ice storm. The total number of hemlock pixels classified in the 1997–1998 aerial image pair decreased 1.8%; the total number of hemlock pixels classified in the 1998–1999 image pair increased over 12% (Fig. 2).

Table 2
Hemlock population matrices derived from ground data sets

Stage at time $t+1$	Stage at time t					
	1	2	3	4	5	6
1997–1998						
1	0.9030	0	0.2987	0.7711	1.9562	6.0051
2	0.0038	0.9572	0	0	0	0
3	0	0.0120	0.9605	0	0	0
4	0	0	0.0132	0.9712	0	0
5	0	0	0	0.0096	0.9493	0
6	0	0	0	0	0.0217	0.9844
1998–1999						
1	0.9030	0	0.2993	0.7772	1.9585	6.0451
2	0.0038	0.9642	0	0	0	0
3	0	0.0125	0.9704	0	0	0
4	0	0	0.0215	0.9807	0	0
5	0	0	0	0.0145	0.9774	0
6	0	0	0	0	0.0150	0.9962

Table 3
Population characteristics predicted from aerial derived matrices

	1997–1998					1998–1999				
λ	1.0119***					1.0962***				
Stage at time *t*	**1**	**2**	**3**	**4**	**5**	**1**	**2**	**3**	**4**	**5**
Stable stage distribution	0.1131	0.1450	0.3124	0.2210	0.2085	0.0978	0.1390	0.2411	0.2700	0.2521
Reproductive values	1.0000	1.4844	2.1207	2.7201	3.6663	1.0000	1.6667	1.9035	2.3464	2.9950
Elasticities										
Satge at time *t* + 1										
1	0.0179	0.0079	0.0073	0.0076	0.0073	0.0133	0.0056	0.0051	0.0072	0.0138
2	0.0137	0.0479	0.0182	0.0057	0.0058	0.0135	0.0458	0.0226	0.0081	0.0164
3	0.0131	0.0317	0.1671	0.0543	0.0150	0.0066	0.0328	0.1104	0.0458	0.0151
4	0.0034	0.0038	0.0797	0.1363	0.0319	0.0081	0.0157	0.0545	0.1685	0.0442
5	0	0	0.0089	0.0511	0.2644	0.0035	0.0066	0.0182	0.0614	0.2572

*** Significant difference between λ's, $P < 0.001$.

Table 4
Population characteristics predicted from ground derived matrices

	1997–1998						1998–1999					
λ	0.9944**						1.0093**					
Stage of time *t*	**1**	**2**	**3**	**4**	**5**	**6**	**1**	**2**	**3**	**4**	**5**	**6**
Stable stage distribution	0.8530	0.0871	0.0308	0.0174	0.0037	0.0080	0.8684	0.0732	0.0236	0.0177	0.0080	0.0092
Reproductive values	1.00	24.1	74.7	169.9	331.0	597.4	1.00	28.0	100.8	168.4	279.3	461.9
Elasticities												
Stage at time *t* + 1												
1	0.0545	0	0.0007	0.0009	0.0005	0.0034	0.0526	0	0.0005	0.0009	0.0011	0.0037
2	0.0055	0.1418	0	0	0	0	0.0062	0.1324	0	0	0	0
3	0	0.0055	0.1563	0	0	0	0	0.0062	0.1545	0	0	0
4	0	0	0.0049	0.2030	0	0	0	0	0.0057	0.1958	0	0
5	0	0	0	0.0039	0.0823	0	0	0	0	0.0048	0.1471	0
6	0	0	0	0	0.0034	0.3333	0	0	0	0	0.0037	0.2849

** Significant difference between λ's, $P < 0.01$.

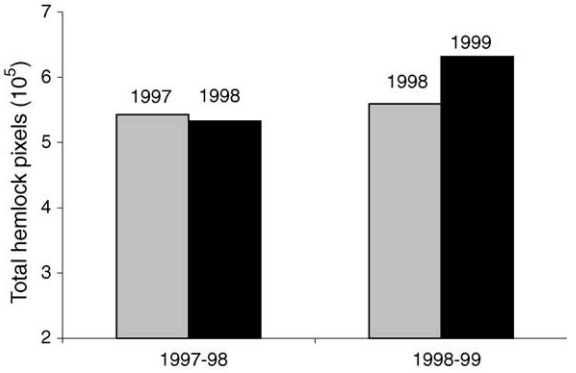

Fig. 2. Comparison of total hemlock pixels classified from the aerial imagery, 1997–1998 and 1998–1999 image pairs.

Between the 1997 and 1998 censuses, ground censusing revealed the death of 38 hemlocks (dbh $\geq$ 5.0 cm), while measurements of crown density found a net of 137 hemlock crowns dropping at least one density class including 13 crowns belonging to dominant, upper canopy trees (Fig. 3). In contrast, from the 1998 to 1999 census, a net of 18 hemlock crowns increased to a higher density class.

The hemlock population, modeled using ground and aerial data, can be represented as life cycle graphs (Fig. 4). Several of the differences between the contrasting collection methods are illustrated by these life cycle graphs and from visual inspection of the matrix population models constructed from the 1997 to 1998 and 1998 to 1999 data sets. The most obvious

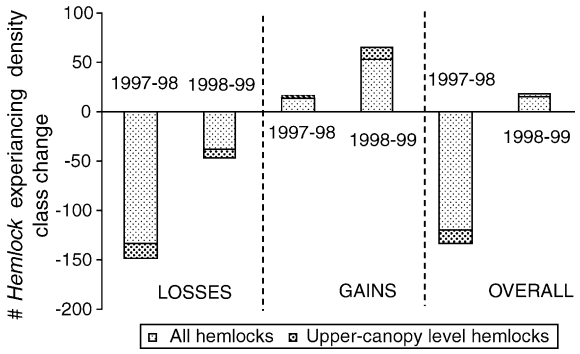

Fig. 3. Hemlock canopy density changes between 1997–1998 and 1998–1999, ground data.

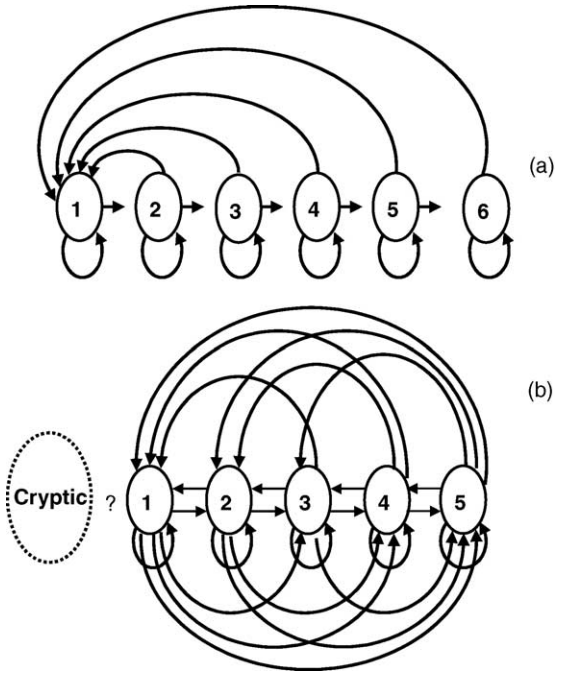

Fig. 4. Life cycle of (a) individuals censused from ground and (b) blobs censused from aerial imagery.

difference was the inability of remote sensing to detect all portions of the population. These cryptic (i.e. hidden from view) individuals in the hemlock population have been quantitatively described previously (Lamar, 2003). Nearly 90% of the small hemlocks (dbh 5–15 cm) were not detected on the aerial imagery. In addition to size, crown density and crown position in the canopy also influenced detection; hemlock with sparse and/or suppressed crowns were more likely to remain undetected from the air. While cryptic individuals exist in many demographic studies, the inability to census individuals that form a major class within a population can influence and, perhaps prevent the meaningful projection of any future population conditions. To investigate the impact of crypticity on overall population growth rate of the hemlock population, we created a series of simulated populations from the complete ground data. Partially cryptic populations were created by setting a threshold ''visibility'' size and removing all individuals smaller than this threshold from analysis. Different threshold sizes were used and four partially cryptic populations created, emulating ground populations missing all individuals from size class 1, size classes 1 and 2, size classes 1–3, and size classes 1–4. Matrix models were constructed and analyzed from these simulated populations. As with the aerially sampled population, the removal of individuals from the ground population resulted in a change in the definition of ''newborn'' hemlocks. Newborn hemlocks were redefined as individuals that had grown into the smallest ''visible'' size class at time $t + 1$. Fertility probabilities, thus, represented the product of numerous actual, yet hidden life cycle transitions including fertility and survival of the newborn until its emergence into the ''visible'' population. Table 5 shows the overall population growth rate of these partially cryptic populations. None of these simulated populations had

Table 5
Effect of simulations of different levels of crypticity on overall population growth rate using data sets modified from ground data

Matrix	λ (1998–1999)	1998–1999
Actual ground population (6 × 6 matrix)	0.9944	1.0093
Size classes 2–6 only (5 × 5 matrix)	0.9896	1.0079
Size classes 3–6 only (4 × 4 matrix)	0.9896	1.0052
Size classes 4–6 only (3 × 3 matrix)	0.9921	1.0104
Size classes 5–6 only (2 × 2 matrix)	0.9910	1.0091

a λ that was significantly different from the λ of the complete ground population in 1997–1998 and 1998–1999, and regardless of the level of simulated crypticity, the small difference in λ between years remained evident.

Another difference in censusing methods, illustrated by the life cycle graphs and matrices, was the greater number of potential transitions between stage classes in the aerial censused population in comparison to the ground censused population. These additional transitions were partly due to the different hemlock characteristics sampled by the two methods. On the ground, the dbh of hemlock trees was measured. The matrices derived from ground-based data looked as expected for a long-lived, low disturbance tree species: low rates of mortality, no regression into smaller size classes, and little growth to larger size classes (Hartshorn, 1975; Enright and Ogden, 1979; Platt et al., 1988). From the aerial imagery, the visible canopy area of hemlock blobs was measured. Unlike dbh measurements, changes in visible canopy area can potentially be much more dynamic. Crown regression, due to a number of environmental influences, is a common and readily detected characteristic. Although growth of canopy area is relatively gradual, visible canopy area growth, from an aerial perspective, can be rapid due to the demise of neighboring crowns and the opening of nearby gaps in the forest canopy. These visible changes would tend to have a real and important impact on the population's future.

Not all changes in the visible canopy would be expected to have such a genuine effect on the population's future. Some movements between aerial matrix elements were, undoubtedly, pseudo-transitions caused by uncorrected distortion differences between images. Distortions are inherent in the process of collecting low elevation, aerial imagery and it is unrealistic to expect to eliminate all the resultant errors. Several steps were taken to minimize these errors so that the pseudo-transitions did not mask the detection of actual change between images. Image to image geometric registration of image pairs resulted in a difference in spatial registration between images, as described by root mean square (RMS) error, of 2.8 pixels (∼36 cm) for the 1998–1999 image pair and 2.6 pixels (∼34 cm) for the 1997–1998 image pair (Lamar et al., 2004).

To further reduce the effects of distortion differences between image pairs, an automated blob reconciliation procedure was utilized to resolve classification differences using a ''best-fit'' approach with re-assignment of ''cross identified'' areas to the same hemlock blob for comparable time periods; thus, ensuring the meaningful comparison of multi-temporal data sets. It was possible, however, that, because of uncorrected distortion differences between years, some small portions of actual hemlock crowns, when viewed from the air, could have been represented by completely unique pixel sets on the multitemportal imagery. In that case, even following automated reconciliation, a crown portion could be assigned, as viewed from time t, to Blob A and the same crown portion as viewed from time $t + 1$ could be assigned to Blob B. The result of the switched assignments would be a pair of pseudo-transitions, a reduction in size for Blob A and an increase in size for Blob B over time and a possible change of size classes. While a significant number of the same type of pseudo-transitions (for example, individuals ''growing'' from size class 1 to 2) would impact the population projections, given a large enough sample size and the expected similar distribution of individuals on both sides of size class boundaries, we anticipated a balanced number of pseudo-transitions occurring in both directions between adjacent size classes (Fig. 5). Thus, in the previous example, the number of individuals pseudo-regressing from size class 2 to 1 should balance the number of individuals pseudo-growing from size class 1 to 2. The effect of balanced pseudo-transitions on the overall population growth

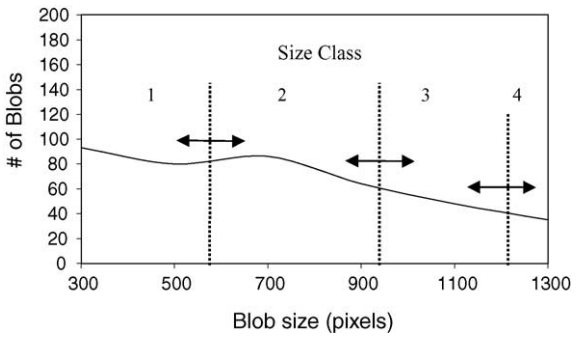

Fig. 5. Blob size distribution, 1997–1998 data set. Note the relative balance between numbers of blobs on either side of category boundaries.

Table 6
Effect of simulations of added balanced transitions between size classes on overall population growth rate using data set modified from 1998–1999 aerial data

Balanced transitions between size classes	Overall population growth rate (number of balanced transitions added)		
	λ (20)	λ (40)	λ (60)
1–2	1.0950	1.0938	1.0927
2–3	1.0946	1.0931	1.0918
3–4	1.0952	1.0944	1.0936
4–5	1.0968	1.0975	1.0982

λ for actual population = 1.0962. No significant difference found between λ of actual population and λ's of populations with added transitions (P, in all cases, $\geq$0.397).

rate was investigated by creating a series of simulated populations. Each simulated population consisted of the original aerial data plus a specified number of additional blobs, an equal number of which were allowed to grow or regress into adjacent size classes between times t and $t + 1$. An additional 20, 40, or 60 blobs were added to the simulated populations, half of the blobs were grown into the next larger size class, and half of the blobs were regressed from that size class into the next smaller size class. The addition of pseudo-transitions, even simulations with 60 new blobs added to the population and allowed to grow and regress between size classes 1 and 2, 2 and 3, 3 and 4, or 4 and 5, had no significant effect on overall population growth rate (Table 6). We thus could reasonably assume that significant differences between matrix projections derived from aerial imagery were not due to balanced transitions between adjacent size classes but real directional changes in the visible canopy area of blobs.

Another distinctive characteristic of matrices derived from aerial imagery was the merger of two population attributes into one transition element. For example, in Table 1, transitions involving the movement of blobs from the larger classes into size class 1 (a_{1j}, where $j > 1$), a transition that often is associated exclusively with fertility, consisted of both a fertility component and a size regression component. Similarly, transition a_{24}, typically a transition describing regression, was comprised of both a regression and fertility component. This 2-component transition often is seen in demographic models of plant parts (McGraw, 1989), but less frequently in models of long-lived genets.

4. Discussion

Censusing a plant population by remote sensing revealed many differences from the traditional ground-based demographic approach. Numerically, a large part of the hemlock population was invisible in the aerial imagery. Most of these hidden trees were small, understory and/or sparsely foliated individuals (Lamar, 2003). By establishing a threshold blob size for the visible segment of the population, additional, mostly small trees were eliminated from demographic analysis. Cryptic individuals are not uncommon in traditional plant demography. For example, seeds in the soil or dormant but living individuals are frequently present in plant populations but not censused directly. In any population model, the consequences of ignorance of a portion of the population should be considered. Treating the missing portion as a "black box" could affect model predictions significantly, particularly if the behaviors in that life stage are critical. By simulating a series of partially cryptic populations from the complete ground data, we found that the elimination of hemlock seedling and smaller trees from analysis had no significant effect on overall population growth rate. Over a long time period, large changes to the invisible fraction within the seed, seedling and small sapling stages can, obviously, have an important impact on the hemlock population and the incomplete sampling of these stages may significantly delay the detection of these impacts (until the effect of these changes becomes measurable in the visible portion of the population). Nevertheless, the insignificant effect of seedling/small hemlock crypticity on overall population growth rate, indicates that, for many monitoring purposes, censusing only the portions of a population making large "contributions" to λ can accurately represent overall population dynamics.

Two of the most important components of the hemlock population were visible and censused in the aerial sampling: large upper canopy hemlock trees and smaller trees located in canopy gaps or under lightly branched overstory trees (Lamar, 2003). Large adult trees have been shown to have a disproportionately high influence on the future dynamics of a population (Hartshorn, 1975; Enright and Ogden, 1979). Small hemlocks located within a gap or higher light environment have been found to experience rapid

increases in height and lateral branch growth (Hibbs, 1982). Hemlock ring widths show evidence of many release and suppression events and it is likely that multiple disturbance episodes are often needed for the trees to grow into the upper canopy (Oliver and Stephens, 1977). It is thus expected that small visible trees in the study plot would be more likely to reach the upper canopy layer, and thus, contribute more to future population growth than trees of similar size hidden from aerial censusing.

The calculation of fertility probabilities offered another example of the different perspectives provided by remote sensing and traditional ground sampling. In the case of measuring fertility, both perspectives offered advantages and disadvantages. The spatially explicit nature of the remotely sensed data permitted the addition of a distance function when calculating individual fertility, adding an element of biological realism not available from most ground derived demographic data. On the other hand, the necessity of defining aerial ''newborns'' as newly visible blobs within the forest canopy meant the ''newborn'' might be several years to decades old and the actual parents may be no longer surviving at the time of the parental census. This could lead to a greater inherent statistical error in calculating fertilities than is found in traditional demographic studies. The division of the aerial censused population into blobs rather than true individual crowns also loses the advantage of population units with genetic identity that often (though not always) accompanies traditional censusing techniques.

Blobs and individuals, however, share many population characteristics; the advantages of one sampling perspective over another are often not distinct. Indeed, the majority of blobs (~70%) showed a 1:1 correspondence with actual tree crowns (Lamar et al., 2004). Ultimately, changes in size structure and abundance of individuals is likely to be reflected in blob sizes and numbers. Importantly from an ecological perspective, the tree component comprising blobs and those comprising tree individuals, both, can influence their surrounding environments and compete for resources with their neighbors. The cost-effectiveness of sampling large numbers of spatially explicit blobs over large geographic areas is a distinct advantage of aerial sampling, with this advantage becoming greater the larger the censused populations.

Until remote sensing instruments can detect individuals with the same resolution and angular mobility as the human eye, the census data extracted from these instruments will differ in several respects. The important question is: Does the perspective from the air yield benefits in terms of detecting population change and identifying the causes of this change? This particular study, which is the first to attempt to answer this question in the context of demographic modeling, suggests the answer is an equivocal yes. Both ground and aerial data showed significant increases in λ between the 1997–1998 and 1998–1999 matrices. The change in λ was much greater for the aerial derived matrices, and indeed, we would not expect ground measurements of dbh to detect many of the sub-lethal crown disturbance events that resulted from the February 1998 ice storm. Other data from the air (total hemlock pixels) and ground (crown density class) supported the idea that a real change in population status occurred.

Although the pattern of crown density class measurements showed distinct changes between 1997–1998 and 1998–1999, supporting the findings of the aerial derived matrices, a direct comparison of an individual tree's ground derived, crown density and a blob's aerial derived, visible canopy area must be made cautiously. Not only should simply the different perspective of the two measurements be expected to cause variability, but the ground measurements also fail to consider the effects of crown damage to neighboring non-hemlock components of the forest and the resulting canopy openings. A National Park Service (NPS) survey following the 1998 ice storm showed 11.3% of the live trees sampled in upper elevation plots suffered crown damage (Cass, 1999). Oaks (*Quercus* sp.) and red maple (*Acer rubrum*) were the most severely damaged species. The numerous canopy openings that formed within the study plot following the ice storm provided an indirect positive impact on the lower canopy level hemlocks. This benefit helped to balance the direct negative impact of the storm on hemlock and explains why, although a net of 137 hemlocks (~10% of the population) dropped at least one density class between the 1997 and 1998 censuses, total hemlock pixels measured from the air only dropped 1.8% and λ derived from the aerial imagery actually remained slightly >1.0. The direct

negative impacts of the storm on hemlock were apparently balanced by the indirect positive impacts caused by the many canopy openings.

Following this disturbance event, the response of hemlock between 1998 and 1999 was more pronounced in the aerial imagery (both total hemlock pixels and λ) than ground derived crown density measurements. From 1998 to 1999, the number of hemlock pixels within the imagery increased over 12%, overall population growth rate, derived from the aerial matrix, increased over 9% yet, only a net of 18 hemlocks increased at least one density class. It is quite possible that the broad boundaries of the density classes failed to detect many additional small increases in crown density.

The fact that a similar population trend could be inferred from both ground and aerial data represents a positive step forward in the use of remote sensing for population monitoring. Future improvements in sensor technology will make remote sensing even more valuable to plant population studies. Other types of remote sensors, such as lidar and radar profiling instruments, may prove particularly useful for the improved detection of small, hidden individuals that were not detectable in this study (Næsset and Økland, 2002; Brandtberg et al., 2003). Lidar imagery may also provide a more accurate view into areas obscured by shadows on other imagery. One of the reasons hemlock was selected for this study was that it is spectrally distinctive in the hardwood forest context. However, the inability of the spectral segmentation procedure to distinguish hemlock from other evergreen species meant that our ''population'' of 497–666 blobs was not exclusively hemlock, but actually included one adult white pine, one adult red spruce, and four clumps of mountain laurel. While the impact of spectral inseparability was lessened in the study plot since ~97% of the evergreen component was hemlock, future investigations in more diverse communities will require improved species separability. The coarse spectral resolution of the sensor contributed to our inability to distinguish hemlock. Current and forthcoming sensors with increased spectral resolution combined with radiometric enhancement techniques offer much promise for future spectral segmentation at a species level (Key et al., 2001; May et al., 2003). The incorporation of other environmental information (aspect, soil type, and elevation) within a GIS framework could also enhance species separability.

Continued improvements in spectral and spatial resolution should allow ecologists to collect even more detailed population data over larger regional and even sub-continental scales. The cost effectiveness of remote sensing should increase the ability to provide basic demographic information on species of conservation concern. In addition, the ability to follow 100,000's of spatially explicit individual population units over time within a regional landscape provides many new opportunities for demographic study. For example, by structuring the remotely sensed population by both size and the density of local neighborhoods, the effect of density dependence within a population can be investigated. Overlaying the population information with other layers of spatially explicit environmental data such as soil maps, elevation maps, and surface water maps within a GIS framework allows the investigation of the influence of both local and regional environmental variables on population dynamics. The marriage of remote sensing techniques, GIS analysis and demographic ecological studies promises to answer many fundamental ecological questions, heretofore intractable, regarding the factors that determine population structure and dynamics.

Acknowledgments

This work was supported by a NSF ESPCoR grant and NSF grant DBI-9808312. We would like to thank Timothy Warner, Charles Yuill, William Peterjohn, and Richard Thomas for their comments on the initial manuscript.

References

Allphin, L., Harper, K.T., 1997. Demography and life history characteristics of the rare kechina daisy (*Erigeron kechinensis*, Asteraceae). Am. Midland Nat. 138, 109–120.

Baptista, W.B., Plat, W.J., Macchiavelli, R.C., 1998. Demography of a shade-tolerant tree (Fagus grandifolia) in a hurricane-disturbed forest. Ecology 79, 38–53.

Brandtberg, T., Warner, T., Landenberger, R., McGraw, J., 2003. Detection and analysis of individual leaf-off tree crowns in small footprint, high sampling density lidar data from the eastern

deciduous forest in North America. Remote Sens. Environ. 85, 290–303.

Busing, R.T., 1995. Disturbance and the population dynamics of *Liriodendron tulipifera*: simulations with a spatial model of forest succession. J. Ecol. 83, 45–53.

Cass, W., 1999. Severity of ice damage to chestnut oak forest within Shenandoah National Park. In: Shenandoah National Park Resource Management Newsletter, .

Caswell, H., 2001. Matrix Population Models. Sinauer Associates, Inc., Sunderland, MA.

Clark, J.S., Macklin, M., Wood, L., 1998. Stages and spatial scales of recruitment limitation in southern Applacachian forest. Ecol. Monogr. 68, 213–235.

Clark, J.S., Silman, M., Kern, R., Macklin, E., HilleRisLambers, L., 1999. Seed dispersal near and far: patterns across temperate and tropical forests. Ecology 80, 1475–1494.

Davelos, A.L., Jarosz, A.M., 2004. Demography of American chestnut populations: effects of a pathogen and a hyperparasite. J. Ecol. 92, 675–685.

Dunning, J.B., Stewart, D.J., Danielson, B., Noon, B.R., Root, T.L., Lamberson, H., Stevens, E.E., 1995. Spatially explicit population models: current forms and future uses. Ecol. Monogr. 5, 3–11.

Enright, N., Ogden, J., 1979. Applications of transition matrix models in forest dynamics: *Araucaria* in Papua New Guinea and *Nothofagus* in New Zealand. Aust. J. Ecol. 4, 3–23.

Erikson, M., 2003. Segmentation of individual tree crowns in colour aerial photographs using region growing supported by fuzzy rules. Can. J. Forest Res. 33, 1557–1563.

Freckleton, R.P., Silva Matos, D.M., Bovi, L.A., Watkinson, A.R., 2003. Predicting the impacts of harvesting using structured population models: the importance of density-dependence and timing of harvest for a tropical palm tree. J. Appl. Ecol. 40, 846–858.

Godman, R.M., Lancaster, L., 1990. *Tsuga canadensis*. Silvics of North America. USDA Forest Service Agricultural Handbook, vol. 654, pp. 604–612.

Golubov, J., Mandujano, M.D., Franco, M., Montana, C., Eguiarte, L.E., Lopez-Portilla, J., 1999. Demography of the invasive woody perennial *Prosopis glandulosa* (Honey mesquite). J. Ecol. 87, 955–962.

Gougeon, F.A., 1995. A crown-following approach to the automatic delineation of individual tree crowns in high spatial resolution aerial images. Can. J. Remote Sens. 21, 274–284.

Graetz, R.D., 1990. Remote sensing of terrestrial ecosystem structure: an ecologist's pragmatic view. In: Hobbs, R.J., Mooney, H.A. (Eds.), Remote Sensing of Biosphere Functioning. Springer-Verlag, New York, pp. 7–30.

Greene, D.F., Canhan, C.D., Coates, K.D., Lepage, P.T., 2004. An evaluation of alternative dispersal functions for trees. J. Ecol. 92, 758–766.

Guardia, R., Raventos, J., Caswell, H., 2000. Spatial growth and population dynamics of a perennial tussock grass (*Achnatherum calamagrostis*) in a badland area. J. Ecol. 88, 950–963.

Hall, F.G., Botkin, D.B., Strebel, D.E., Woods, K.D., Goetz, S.J., 1991. Large-scale patterns of forest succession as determined by remote sensing. Ecology 72, 628–640.

Harper, J.L., 1976. The concept of population in modular organisms. In: May, R.M. (Ed.), Theoretical Ecology. Principles and Applications. Blackwell Scientific Publications, Oxford, pp. 53–77.

Harper, J.L., 1977. Population Biology of Plants. Academic Press, San Diego, CA.

Hartshorn, G.S., 1975. A matrix model of tree population dynamics. In: Golley, F.B., Medina, E. (Eds.), Tropical Ecological Systems. Springer-Verlag, New York, pp. 41–51.

Hibbs, D.E., 1982. Gap dynamics in a hemlock-hardwood forest. Can. J. Forest Res. 12, 522–527.

Huenneke, L.F., Marks, P.L., 1987. Stem-dynamics of the shrub *Alnus incanta* ssp. *rugosa*: transition matrix models. Ecology 68, 1234–1242.

Kaye, T.N., Pendergrass, K.L., Finley, K., Kauffman, J.B., 2001. The effect of fire on the population viability of an endangered prairie plant. Ecol. Appl. 11, 1366–1380.

Key, T., Warner, T.A., McGraw, J., Fajvan, M.A., 2001. A comparison of multispectral and multitemporal information in high spatial resolution imagery for classification of individual tree species in a temperate hardwood forest. Remote Sens. Environ. 100–112.

Kramer, H.J., 2002. Observation of the Earth and its Environment—Survey of Missions and Sensors. Springer-Verlag.

Lamar, W.R., 2003. Censusing and modeling a population of eastern hemlock (*Tsuga canadensis* L.) using remote sensing. Ph.D. West Virginia University, Morgantown, WV.

Lamar, W.R., McGraw, J., Warner, T., 2004. Multitemporal censusing of a population of eastern hemlock (*Tsuga canadensis* L.) from remotely sensed imagery using an automated segmentation and reconciliation procedure. Remote Sens. Environ. 94, 133–143.

Lefkovich, L.P., 1965. The study of population growth in organisms grouped by stages. Biometrics 21, 1–18.

May, D.Z., Brown, D.J., Bohlman, S.A., 2003. Evaluation of high-resolution, multi-band imagery for determining proportions of oak and maple LAI in Black Rock Forest, NY. In: 88th Annual Meeting, The Ecological Society of America, p. 221.

McGraw, J.B., 1989. Effects of age and size on life histories and population growth of *Rhododendron maximum* shoots. Am. J. Bot. 76, 113–123.

Menges, E.S., 1990. Population viability analysis for an endangered plant. Conserv. Biol. 4, 52–62.

Moloney, K.A., 1986. A generalized algorithm for determining category size. Oecologia 69, 176–180.

Næsset, E., Økland, T., 2002. Estimating tree height and tree crown properties using airborne scanning laser in a boreal nature reserve. Remote Sens. Environ. 79, 105–115.

Niemann, K.O., 1995. Remote sensing of forest stand age using airborne spectrometer data. Photogramm. Eng. Remote Sens. 61, 1119–1127.

Oliver, C.D., Stephens, E.P., 1977. Reconstruction of a mixed-species forest in central New England. Ecology 58, 562–572.

Pacala, S.W., 1989. Plant population dynamic theory. In: Roughgarden, J., May, R., Levine, S. (Eds.), Perspectives in Ecological Theory. Princeton University Press, Princeton, pp. 54–67.

Pacala, S.W., Canham, C.D., Saponara, J., Silander Jr., J.A., Kobe, R.K., Ribbens, E., 1996. Forest models defined by field mea-

surements: estimation, error analysis and dynamics. Ecol. Monogr. 66, 1–43.

Parker, I.M., 2000. Invasion dynamics of Cytidud dcoparius. A matrix model approach. Ecol. Appl. 10, 726–743.

Pinero, D., Martinez-Ramos, M., Sarukhan, J., 1984. A population model of *Astrocaryum mexicanum* and a sensitivity analysis of its finite rate of increase. J. Ecol. 72, 977–991.

Platt, W.J., Evans, G.W., Rathburn, S.L., 1988. The population dynamics of a long-lived conifer (*Pinus palustris*). Am. Nat. 131, 1794–1806.

Ribbens, E., Silander, J.J.A., Pacala, S.W., 1994. Seedling recruitment in forests: calibrating models to predict patterns of tree seedling dispersion. Ecology 75, 1794–1806.

Shugart, H.H., Smith, T.M., 1992. The potential for application of individual-based simulation models for assessing the effects of global change. Annu. Rev. Ecol. Syst. 23, 15–38.

Silvertown, J., Franco, M., Menges, E., 1996. Interpretation of elasticity matrices as an aid to the management of plant populations for conservation. Conserv. Biol. 10, 591–597.

Silvia, J.F., Raventos, J., Caswell, H., Trevisan, M.C., 1991. Population responses to fire in a tropical savanna grass. J. Ecol. 79, 345–355.

Wulder, M., Niemann, K.O., Goodenough, D.G., 2000. Local maximum filtering for the extraction of tree locations and basal area from high spatial resolution imagery. Remote Sens. Environ. 73, 103–114.